*Inorg. Chem.* **2006**, *45*, 3113–3123


# Biologically Relevant Phosphoranes: Structural Characterization of Glucofuranose- and Xylofuranose-Based Phosphoranes[1]

**Natalya V. Timosheva, A. Chandrasekaran, and Robert R. Holmes***

*Department of Chemistry, University of Massachusetts, Amherst, Massachusetts 01003-9336*

Received December 8, 2005

Carbohydrate-based phosphoranes were synthesized by reacting 2,2′-ethylidenebis(4,6-di-*tert*-butylphenyl)-fluorophosphite with 1,2-O-isopropylidene-α-D-glucofuranose, β-chloralose, and 1,2-isopropylidene-α-D-xylofuranose to form the monocyclic biophosphoranes **1**–**3**, respectively, in the presence of N-chlorodiisopropylamine. Synthesis of the monocyclic biophosphorane **4** was achieved by reacting tris(2,6-di-isopropylphenyl)phosphite with 1,2-O-isopropylidene-α-D-glucofuranose in the presence of N-chlorodiisopropylamine. X-ray analysis of **1**–**4** revealed trigonal bipyramidal structures with the carbohydrate components occupying axial–equatorial sites. An eight-membered ring in **1**–**3** occupied diequatorial sites of the trigonal bipyramid. Solution and solid state $^{31}$P and solution $^{19}$F, $^{1}$H, and $^{13}$C NMR measurements including variable temperature and correlation spectroscopy studies established retention of the solid state structure in solution. A dynamic equilibrium exists among two isomeric forms. These biophosphoranes serve as models for active sites of phosphoryl transfer enzymes. The rapid exchange process reorients the carbohydrate component of the trigonal bipyramidal phosphorane. At an active site, this type of pseudorotational behavior provides a mechanism that could bring another active site residue into play and account for a means by which some phosphoryl transfer enzymes express promiscuous behavior.

## Introduction

Pentacoordinate phosphorus is considered to be an intermediate or transition state in the formation or hydrolysis of biologically relevant phosphorus compounds such as DNA, RNA, and c-AMP.[2] It is our contention that residues at active sites of phosphoryl transfer enzymes are capable of entering into donor interaction at the pentacoordinate phosphorus atom and, as a consequence, assist in nucleophilic attack.[2] Toward that goal, we have studied donor coordination in a variety of environments that mimic active sites, including anionicity, hydrogen bonding,[3,4] packing effects,[5] that is, van der Waals forces, the pseudorotational problem,[6,7] and the ease with which the phosphorus atom undergoes coordination changes.[8] Recent work on enzyme promiscuity[9−12] and moonlighting activities[13−16] also has been considered.

To model active site interactions of phosphoryl transfer enzymes more closely, we now have turned our attention to

* Author to whom correspondence should be addressed. Phone: (413) 687-3918. Fax: (413) 545-4490. E-mail: rrh@chem.umass.edu.

(1) (a) Pentacoordinated Molecules, part 143. (b) Part 142: Timosheva, N. V.; Chandrasekaran, A.; Holmes, R. R. *J. Am. Chem. Soc.* **2005**, *127*, 12474−12475.
(2) Holmes, R. R. *Acc. Chem. Res*. **2004**, *37*, 746−753; **1998**, *31*, 535−542 and references therein.
(3) Chandrasekaran, A.; Day, R. O.; Holmes, R. R. *Inorg. Chem*. **2001**, *40*, 6229−6238.
(4) . Chandrasekaran, A.; Day, R. O.; Holmes, R. R. *Inorg. Chem*. **2002**, *41*, 1645−1651
(5) Chandrasekaran, A.; Timosheva, N. V.; Day, R O.; Holmes, R. R. *Inorg. Chem*. **2003**, *42*, 3285−3292.
(6) Holmes, R. R. *Pentacoordinated Phosphorus − Structure and Spectroscopy*; American Chemical Society: Washington, D. C., 1980; Vol. I, ACS Monograph 175, p 479.
(7) Holmes, R. R. *Pentacoordinated Phosphorus − Reaction Mechanisms*; American Chemical Society: Washington, D. C., 1980; Vol. II, ACS Monograph 176, p 237.
(8) Timosheva, N. V.; Chandrasekaran, A.; Day, R. O.; Holmes, R. R. *J. Am. Chem. Soc.* **2002**, *124*, 7035−7040.
(9) O'Brien, P. J.; Herschlag, D. *Chem. Biol.* **1999**, *6*, R91−105.
(10) James, L. C.; Tawfik, D. S. *Protein Sci.* **2001**, *10*, 2600−2607.
(11) Schmidt, D. M. Z.; Mundorff, E. C.; Dojka, M.; Bermundez, E.; Ness, J. E.; Govindarajan, S.; Babbitt, P. C.; Minshull, J.; Gerlt, J. A. *Biochemistry* **2003**, *42*, 8387−8393.
(12) Seffermick, J. L.; Wackett, L. P. *Biochemistry* **2001**, *40*, 12747−12753.
(13) (a) James, L. C.; Roversi, P.; Tawfik, D. S. *Science* **2003**, *299*, 1362−1367. (b) James, L. C.; Tawfik, D. S. *Trends Biochem. Sci.* **2003**, *28*, 361−368. These two articles describe the conformational diversity of enzymes. The latter reference lists a glossary of terms used to describe the ability of a protein to exhibit more than one specificity or perform more than one function.
(14) Copley, S. D. *Curr. Opin. Chem. Biol.* **2003**, *7*, 265−272. This reference also gives examples of four types of catalytic promiscuity.
(15) Jeffrey, C. J. *Trends Biochem. Sci.* **1999**, *24*, 8−11.
(16) Moonlighting proteins, a term coined by Gregory A. Petsko, is discussed also by Yarnell, A. *Chem. Eng. News* **2003**, *81* (49), 33−35.

10.1021/ic052105e CCC: $33.50 
Published on Web 02/24/2006

**Scheme 1**

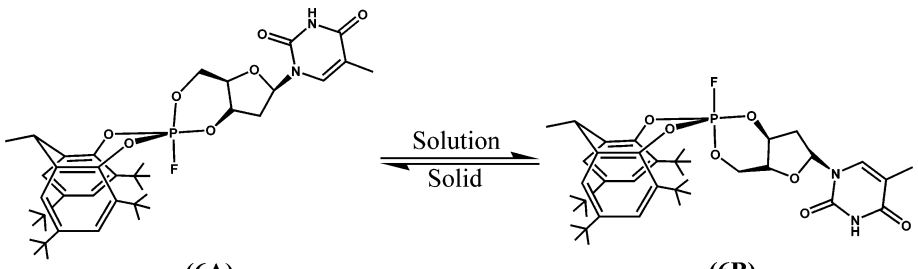


**(6A)**
**X-Ray Structure**

**(6B)**

constructing biologically relevant phosphorus compounds. We note that, although hundreds of penta- and hexacoordinate phosphoranes have been structurally characterized, no phosphorane with a biological component has been structurally characterized despite work in this area over the past 30 years or so. However, in a recent communication, we reported the first structural characterization of two phosphoranes, one with a nucleoside and one with a carbohydrate moiety (Scheme 1 shows the thymidine phosphorane).[1b] We were able to accomplish this goal by using systems that improved the solubility, stability, and crystallizability of the phosphorane.[1b] Herein, we extend that work in which bicyclic and monocyclic phosphoranes containing glucofuranose and xylofuranose derivatives are studied.

## Experimental Section

2,2′-Ethylidenebis(4,6-di-*tert*-butylphenyl)fluorophosphite (technical grade; **A**), 1,2-O-isopropylidene-α-D-glucofuranose (gf-ip-$H_2$; **B**), *β*-chloralose (gf-chloral-$H_2$; **C**), and 1,2-isopropylidene-α-D-xylofuranose (xf-ip-$H_2$; **D**) (all Aldrich) were used as supplied. N-chlorodiisopropylamine[17] was synthesized according to our earlier methods. Solvents were purified according to standard procedures.[18] All of the reactions were carried out in an argon atmosphere. The solution NMR spectra were recorded on an Avance-400 ($^1$H, $^{13}$C, and $^{31}$P at 400.1, 100.6, and 162.0 MHz, respectively) or Bruker DPX300 FT-NMR ($^{19}$F at 282.4 MHz) spectrometer. Solid state magic angle spinning $^{31}$P NMR were recorded on a Bruker DSX300 FT-NMR (at 121.5 MHz) spectrometer with proton decoupling. Solution fluorine and phosphorus NMR spectra were recorded in the sweep-off mode. Chemical shifts are reported in parts per million; downfield positive; and relative to tetramethylsilane for $^1$H and $^{13}$C, to $CFCl_3$ for $^{19}$F NMR, and to 85% $H_3PO_4$ for $^{31}$P NMR. All were recorded at around 23 °C. The assigned phosphorus couplings are based on the phosphorus-decoupled-proton NMR spectra. The numberings used in $^1$H and $^{13}$C NMR data assignment are the same as those used in X-ray structure determinations. Elemental analyses were performed by the University of Massachusetts Microanalysis Laboratory.

**Syntheses. $CH_3CH[C_6H_2(t\text{-}Bu)_2O]_2PF$(gf-ip) (1).** 2,2′-Ethylidenebis(4,6-di-*tert*-butylphenyl)fluorophosphite **A** (3.00 g, 6.16 mmol) and isopropylidene-glucofuranose **B** (1.35 g, 6.13 mmol) were stirred in dichloromethane (150 mL). N-chlorodiisopropylamine (1.00 mL, 6.78 mmol) was added, and the solution was stirred for 24 h. The solvent was removed, and the residue was extracted with ether (150 mL) and filtered. The solvent was removed from the filtrate and the residue recrystallized from heptane/dichloromethane (60:90 mL) to obtain a fluffy solid. Yield: 1.80 g in two batches (41.6%). mp: 225−228 °C (dec). $^{31}$P NMR ($CH_2Cl_2$): −55.2 (d, 778 Hz), −55.8 (d, 771 Hz) in a 4:5 ratio. $^{31}$P NMR ($CH_3CN$): −54.3 (d, 771 Hz), −55.3 (d, 761 Hz) in a 1:1 ratio. $^{31}$P NMR (toluene, 295 K) −54.1 (d, 786 Hz), −54.6 (d, 781 Hz) in a 1:1 ratio. $^{31}$P NMR (toluene, 333 K): −54.1 (d, 784 Hz). $^{31}$P NMR (solid): −54.9 (d, 811 Hz). $^{19}$F NMR ($CH_2Cl_2$): −41.63 (d, 778 Hz), −42.17 (d, 771 Hz) in a 3:4 ratio. $^{19}$F NMR ($CH_3CN$): −39.65 (d, 771 Hz), −39.64 (d, 761 Hz) in a 1:1 ratio. $^{19}$F NMR (toluene): −39.58 (d, 786 Hz), −40.10 (d, 782 Hz) in a 1:1 ratio. $^1$H NMR ($CDCl_3$, 295 K): 1.29 (s, 18H, *tert*-butyl), 1.34 (s, 3H, $CMe_2$, major), 1.39 (s, br, 18H, *tert*-butyl), 1.41 (s, 3H, $CMe_2$, minor), 1.46 (d, 6.5 Hz, 3H, $Ar_2CMe$, minor), 1.54 (s, 3H, $CMe_2$, major), 1.55 (s, 3H, $CMe_2$, minor), 1.63 (s, water), 1.66 (d, 7.2 Hz, 3H, $Ar_2CMe$), 2.04 (d, 3.0 Hz, OH, minor), 2.95 (d, 3.0 Hz, OH, major), 3.37 (s, br, 1H, $Ar_2CH$, minor), 4.0−4.6 (m, 6H, H on C2−C6), 4.88 (m, br, 1H, $Ar_2CH$, major), 5.98 (d, 2.6 Hz, C1−H, minor), 6.02 (d, 3.3 Hz, C1−H, major), 7.17 (s, br, 2H, aryl-H), 7.396 (s, 1H, aryl-H, major), 7.402 (s, 1H, aryl-H, minor). $^1$H NMR ($CDCl_3$, 223 K): 1.30 (s, br, 18H, *tert*-butyl), 1.36 (s, 3H, $CMe_2$, major), 1.39 (s, br, 12H, *tert*-butyl), 1.40 (s, br, 6H, *tert*-butyl), 1.41 (s, 3H, $CMe_2$, minor), 1.46 (d, 6.1 Hz, 3H, $Ar_2CMe$, minor), 1.57 (s, 3H, $CMe_2$, major), 1.59 (s, 3H, $CMe_2$, minor), 1.67 (d, 6.9 Hz, 3H, $Ar_2CMe$), 2.15 (s, water), 2.67 (d, 4.9 Hz, OH, minor), 3.41 (s, br, 1H, $Ar_2CH$, minor), 3.59 (d, 2.8 Hz, OH, major), 4.1−4.8 (m, 6H, H on C2−C6), 4.88 (m, br, 1H, $Ar_2CH$, major), 6.02 (d, 3.4 Hz, C1−H, minor), 6.09 (d, 3.4 Hz, C1−H, major), 7.18 (br, 2H, aryl-H), 7.41 (s, 1H, aryl-H, major), 7.43 (s, 1H, aryl-H, minor). $^{13}$C NMR ($CDCl_3$) **isomer A (major):** 20.72 (s, $Ar_2CHMe$, C17), 26.07 (s, $O_2CMe_2$), 26.87 (s, $O_2CMe_2$), 30.18 (s, $Ar_2CH$, C16), 30.68 (s, $CMe_3$, closer to P), 31.48 (s, $CMe_3$, far from P), 34.63 (s, $CMe_3$, far from P), 34.96 (s, $CMe_3$, closer to P), 65.19 (s, C6), 66.83 (d, 6.5 Hz, C4 or C2/C3), 74.79 (s, C3 or C2/C4), 81.38 (d, 10.8 Hz, C5), 85.13 (s, C2 or C3/C4), 105.24 (s, C1), 111.91 (s, C7), 121.25 (s, aryl-CH), 122.33 (s, aryl-CH), 138.20 (br), 147.16 (br, P−O−C-aryl); **isomer B (minor):** 19.15 (s, $Ar_2CHMe$, C17), 26.27 (s, $O_2CMe_2$), 30.18 (s, $Ar_2CH$, C16), 30.68 (s, $CMe_3$, closer to P), 31.48 (s, $CMe_3$, far from P), 34.63 (s, $CMe_3$, far from P), 34.96 (s, $CMe_3$, closer to P), 47.34 (s, $O_2CMe_2$?), 61.20 (s, C6), 69.79 (s, C4 or C2/C3), 74.33 (s, C3 or C2/C4), 80.01 (d, 5.4 Hz, C5), 85.24 (s, C2 or C3/C4), 105.24 (s, C1), 112.14 (s, C7), 121.23 (s, aryl-CH), 122.33 (s, aryl-CH), 136.95 (br), 146.66 (br, P−O−C-aryl). Anal. Calcd for $C_{39}H_{58}O_8FP$: C, 66.46; H, 8.29. Found: C, 66.52; H, 8.41. Single crystals suitable for an X-ray study were obtained from hot acetonitrile at atmospheric conditions.

(17) Chandrasekaran, A.; Day, R. O.; Holmes, R. R. *Inorg. Chem.* **1997**, *36*, 2578−2585.

(18) (a) Riddick, J. A.; Bunger, W. B. Organic Solvents. In *Physical Methods in Organic Chemistry*, 3rd ed.; Wiley-Interscience: New York, 1970; Vol. II. (b) Vogel, A. I. *Textbook of Practical Organic Chemistry*; Longman: London, 1978.

**$CH_3CH[C_6H_2(t\text{-}Bu)_2O]_2PF$(gf-chloral) (2).** 2,2′-Ethylidenebis-(4,6-di-*tert*-butylphenyl)fluorophosphite **A** (3.20 g, 6.57 mmol) and $\beta$-chloralose **C** (2.00 g, 6.47 mmol) were stirred in dichloromethane (150 mL). N-chlorodiisopropylamine (1.00 mL, 6.78 mmol) was added, and the solution was stirred for 70 h. The solvent was removed, and the residue was extracted with ether (150 mL) and filtered. The solvent was removed from the filtrate and the residue recrystallized from heptane/dichloromethane (50:50 mL) to obtain a fluffy solid, which was washed with hexanes (50 mL) and dried. Yield: 1.50 g (29%). It was recrystallized from acetone or acetone/ethanol to obtain a crystalline sample. The crystals obtained from acetone had loosely bound acetone solvate, and those obtained from acetone/ethanol had ethanol solvate. mp: 162−165 °C (acetone). $^{31}$P NMR ($CDCl_3$): −57.3 (d, 785 Hz), −57.6 (d, 778 Hz) in a 1:2 ratio. $^{19}$F NMR ($CDCl_3$): −42.26 (d, 785 Hz), −43.01 (d, 779 Hz) in a 1:2 ratio. $^1$H NMR ($CDCl_3$, 295 K), the A/B isomer ratio was 1:0.6 (acetone signal was observed at 2.17 ppm), **isomer A (major):** 1.29 (s, 18H, *tert*-butyl), 1.40 (s, 18H, *tert*-butyl), 1.67 (d, 7.2 Hz, 3H, $Ar_2CMe$), 1.79 (s, water), 3.09 (br, OH), 4.12 (q, 9.3 Hz, 1H), 4.22−4.68 (br, m, 5H), 4.88 (m, br, 1H), 4.98 (d, 3.5 Hz), 5.63 (s, 1H, $Cl_3CH$), 6.32 (d, 3.2 Hz, C1−H, 1H), 7.18 (s, 2H, aryl-H), 7.40 (s, 1H, aryl-H); **isomer B (minor):** 1.29 (s, 18H, *tert*-butyl), 1.39 (s, 18H, *tert*-butyl), 1.67 (d, 7.2 Hz, 3H, $Ar_2CMe$), 1.79 (s, water), 2.67 (br, OH), 4.22−4.68 (br, m, 5H), 4.88 (m, br, 1H), 4.98 (d, 3.5 Hz), 5.63 (s, 1H, $Cl_3CH$), 6.30 (br, C1−H, 1H), 7.18 (s, 2H, aryl-H), 7.41 (s, 1H, aryl-H). Anal. Calcd for $C_{38}H_{53}O_8Cl_3FP\cdot C_3H_6O$: C, 57.78; H, 6.98. Found: C, 57.47; H, 7.32.

**$CH_3CH[C_6H_2(t\text{-}Bu)_2O]_2PF$(xf-ip) (3).** 2,2′-Ethylidenebis(4,6-di-*tert*-butylphenyl)fluorophosphite **A** (2.60 g, 5.72 mmol) and isopropylidene-xylofuranose **D** (1.00 g, 5.26 mmol) were stirred in dichloromethane (150 mL). N-chlorodiisopropylamine (0.80 mL, 5.42 mmol) was added, and the solution was stirred for 24 h. The solvent was removed, and the residue was extracted with ether (200 mL) and filtered. The solution was left for slow evaporation under an argon flow. It gave phosphorane **3** as a crystalline solid. Yield: 3.30 g (91.6%). mp: 235−237 °C (dec). $^{31}$P NMR ($CH_2Cl_2$): −73.9 (d, 762 Hz), −75.5 (d, 763 Hz) in a 4:5 ratio. $^{31}$P NMR ($CH_3CN$): −72.7 (d, 764 Hz), −74.1 (d, 764 Hz) in a 5:6 ratio. $^{31}$P NMR (toluene, 295 K) −73.3 (d, 774 Hz), −74.3 (d, 774 Hz) in a 3:4 ratio. $^{31}$P NMR (toluene, 373 K): −71.5 (d, 778 Hz). $^{31}$P NMR (solid): −71.4 (d, 774 Hz). $^{19}$F NMR ($CH_2Cl_2$): −36.84 (d, 762 Hz), −36.71 (d, 763 Hz) in a 4:5 ratio. $^{19}$F NMR ($CH_3CN$): −34.70 (d, 765 Hz), −34.35 (d, 764 Hz) in a 9:10 ratio. $^{19}$F NMR (toluene): −34.97 (d, 774 Hz), −35.14 (d, 774 Hz) in a 3:4 ratio. $^1$H NMR ($CDCl_3$): 1.282 (s, 9H, *tert*-butyl), 1.284 (s, 9H, *tert*-butyl), 1.286 (s, 9H, *tert*-butyl), 1.289 (s, 9H, *tert*-butyl), 1.35 (s, 3H, $CMe_2$, major), 1.38 (s, 3H, $CMe_2$, minor), 1.390 (s, 9H, *tert*-butyl), 1.405 (s, 9H, *tert*-butyl), 1.412 (s, 9H, *tert*-butyl), 1.417 (s, 9H, *tert*-butyl), 1.54 (s, 3H, $CMe_2$, minor), 1.55 (s, 3H, $CMe_2$, major), 1.66 (d, 3H, 7.4 Hz, $Ar_2CMe$, major), 1.68 (d, 3H, 7.5 Hz, $Ar_2CMe$, minor), 4.10−4.95 (m, 4.5H, H on C2−C5), 4.82 (m, 1H, $Ar_2CH$), 5.07 (t, 4.9 Hz, 0.5H), 6.04 (d, 3.7 Hz, C1H, major), 6.09 (d, 3.6 Hz, C1H, minor), 7.15 (m, 2H, aryl-H), 7.391 (d, 1.8 Hz, 1H, aryl-H), 7.395 (d, 2.0 Hz, 1H, aryl-H), 7.409 (s, 1H, aryl-H), 7.415 (s, 1H, aryl-H). $^{13}$C NMR($CDCl_3$) **isomer A (major):** 20.91 (s, $Ar_2CHMe$, C26), 26.33 (s, $O_2CMe_2$), 26.79 (s, $O_2CMe_2$), 30.14 (s, $Ar_2CH$, C16), 30.60 (s, $CMe_3$, closer to P), 30.65 (s, $CMe_3$, closer to P), 31.49 (s, $CMe_3$, far from P), 34.98 (s, $CMe_3$), 64.57 (d, 7.0 Hz, C5), 76.12 (d, 2.9 Hz, C2 or C4), 81.67 (dd, 7.3, 5.9 Hz, C4 or C2), 83.27 (d, 17.3 Hz, C3), 105.78 (s, C1), 112.37 (s, C7), 121.22 (s, aryl-CH), 121.23 (s, aryl-CH), 122.16 (s, aryl-CH), 122.22 (s, aryl-CH), 136.81 (d, 3.1 Hz, tert-aryl), 136.93 (d, 3.5 Hz, tert-aryl), 137.02 (d, 4.1 Hz, tert-aryl), 137.06 (d, 4.0 Hz, tert-aryl), 146.40 (m, P−O−C-aryl), 146.50 (m, P−O−C-aryl); **isomer B (minor):** 20.91 (s, $Ar_2CHMe$, C26), 26.87 (s, $O_2CMe_2$), 27.42 (s, $O_2CMe_2$), 30.14 (s, $Ar_2CH$, C16), 30.57 (s, $CMe_3$, closer to P), 30.89 (s, $CMe_3$, closer to P), 31.49 (s, $CMe_3$, far from P), 34.61 (s, $CMe_3$), 67.46 (dd, 7.3, 5.1 Hz, C5), 75.77 (s, C2 or C4), 78.50 (d, 6.0, C4 or C2), 86.37 (d, 14.0 Hz, C3), 106.10 (s, C1), 112.75 (s, C7), 121.41 (s, aryl-CH), 121.47 (s, aryl-CH), 122.22 (s, aryl-CH), 122.32 (s, aryl-CH), 137.88 (m, tert-aryl), 138.21 (d, 6.7 Hz, tert-aryl), 147.20 (m, P−O−C-aryl), 147.80 (m, P−O−C-aryl). The ether peaks appear at 15.27 (s, $CH_3$) and 65.83 (s, $CH_2$). Anal. Calcd for $C_{38}H_{56}O_7FP\cdot 0.1C_4H_{10}O$: C, 67.60; H, 8.42. Found: C, 67.67; H, 8.46 (10% ether was also observed in the proton and carbon NMR but could not be located in the X-ray study).

**$[C_6H_3\text{-}2,6\text{-}(i\text{-}Pr)_2O]_3P$(gf-ip) (4).** Phosphite **5** (4.00 g, 7.11 mmol) and isopropylidene-glucofuranose **B** (1.60 g, 7.27 mmol) were stirred in dichloromethane (150 mL). N-chlorodiisopropylamine (1.00 mL, 6.78 mmol) was added, and the solution was stirred for 24 h. The solvent was removed, and the residue was extracted with ether/heptane (80−40 mL) and filtered. The filtrate was left under an argon flow to obtain a crystalline solid. Yield: 3.40 g (64%). mp: 137−145 °C. $^{31}$P NMR ($CDCl_3$): −59.6.$^1$H NMR ($CDCl_3$, 295 K): 1.0−1.2 (br, 36H, $CHCH_3$), 1.25 (s, 3H, $CMe_2$), 1.40 (s, 3H, $CMe_2$), 1.57 (d, 1H, 2.5 Hz, OH), 1.64 (s, water), 3.12 (q, 1H, 7.5 Hz), 3.50 (br, 6H, $CHMe_2$), 3.67 (d, 1H, 6.3 Hz), 3.84 (td, $^3J_{POCH}$ = 9.5, 3.8 Hz, 1H), 4.06 (s, 1H), 4.12 (ddd, $^3J_{POCH}$ = 29.3, 8.8, 6.5 Hz, 1H), 4.36 (d, 3.5 Hz, 1H), 5.74 (d, 3.5 Hz, 1H, C1H), 6.98−7.06 (br, 9H, aryl-H). $^1$H NMR ($CD_2Cl_2$, 296 K): 1.0−1.2 (br, 36H, $CHCH_3$), 1.22 (s, 3H, $CMe_2$), 1.35 (s, 3H, $CMe_2$), 1.56 (s, water), 1.83 (d, 1H, 2.7 Hz, OH), 3.17 (br, m, 1H), 3.48 (br, 6H, $CHMe_2$), 3.61 (dd, 1H, 6.9, 1.9 Hz), 3.83 (td, $^3J_{POCH}$ = 9.5, 3.6 Hz, 1H), 4.02 (br, 1H), 4.12 (ddd, $^3J_{POCH}$ = 28.8, 8.9, 6.6 Hz, 1H), 4.31 (d, 3.6 Hz, 1H), 5.70 (d, 3.6 Hz, 1H, C1H), 6.98−7.08 (br, 9H, aryl-H). $^1$H NMR ($CD_2Cl_2$, 213 K): 0.35 (d, 5.5 Hz, 3H, $CHCH_3$), 0.77 (d, 5.5 Hz, 3H, $CHCH_3$), 0.90 (d, 6.0 Hz, 3H, $CHCH_3$), 0.96 (d, 5.8 Hz, 3H, $CHCH_3$), 1.03 (d, 5.9 Hz, 3H, $CHCH_3$), 1.2−1.5 (br, 15H, $CHCH_3$), 1.23 (s, 3H, $CMe_2$), 1.30 (d, 6.1 Hz, 3H, $CHCH_3$), 1.38 (s, 3H, $CMe_2$), 1.42 (d, 5.8 Hz, 3H, $CHCH_3$), 2.23 (br, 1H), 2.95 (br, m, 1H, $CHCH_3$), 3.08 (s, 1H, OH), 3.43 (br, m, 1H, $CHCH_3$), 3.61 (br, m, 2H, $CHCH_3$), 3.73 (br, s, 1H), 3.80 (br, m, 2H, $CHCH_3$), 3.87 (t, $^3J_{POCH}$ = 9.9 Hz, 1H), 4.14 (dt, 31.9, 7.5 Hz, 1H), 4.24 (s, 1H), 4.38 (d, 3.2 Hz, 1H), 5.75 (d, 3.5 Hz, 1H, C1H), 6.90−7.30 (br, 9H, aryl-H). Anal. Calcd for $C_{45}H_{65}O_9P$: C, 69.21; H, 8.39. Found: C, 69.47; H, 8.42.

**$[C_6H_3\text{-}2,6\text{-}(i\text{-}Pr)_2O]_3P$ (5).**[19] A solution of 2,6-diisopropylphenol (27.0 mL, 145 mmol) and phosphorus trichloride (4.00 mL, 45.8 mmol) in dichloromethane (200 mL) was stirred while a solution of triethylamine (28.0 mL, 200 mmol in 50 mL dichloromethane) was added dropwise over a period of 20 min. The reaction mixture was stirred for a further period of 46 h. The solvent was removed under a vacuum, the residue extracted with hexane (100 mL), and the residue further extracted with additional hexane (2 × 40 mL). The filtered hexane turbid solution was heated to a clear solution and left for crystallization. It gave a crystalline solid, which was washed with hexane. Yield: 20.7 g in three batches (80%). mp: 243−246 °C. $^{31}$P NMR ($CDCl_3$): 146.3.$^1$H NMR ($CDCl_3$, 295 K): 1.08 (d, 36H, 6.9 Hz, $CHCH_3$), 3.45 (septet of doublets, 6H, 6.9 Hz, $^3J_{POCH}$ = 2.0 Hz, $CHMe_2$), 7.10 (s, 9H, aryl-H). Anal. Calcd for $C_{36}H_{51}O_3P$: C, 76.83; H, 9.13. Found: C, 76.88; H, 8.98.

(19) Though phosphite **5** has been used previously, its synthesis or any characterization data was neither provided nor cited. For its use in metal complexes, see: Krause, J.; Cestaric, G.; Haack, K.-J.; Seevogel, K.; Storm, W.; Poerschke, K.-R. *J. Am. Chem. Soc*. **1999**, *121*, 9807−9823. Krause, J.; H. K.-J.; Porschke, K.-R., *Chem. Commun*. **1998**, 1291−1292.

**Table 1.** Crystallographic Data for Compounds **1**−**4**

| compound | **1** | **2**·**acetone** | **3** | **4** |
|---|---|---|---|---|
| formula | $C_{39}H_{58}FO_8P$ | $C_{38}H_{53}O_8Cl_3FP{\cdot}C_3H_6O$ | $C_{38}H_{56}FO_7P$ | $C_{45}H_{65}O_9P$ |
| fw | 704.82 | 852.20 | 674.80 | 780.94 |
| cryst syst | monoclinic | orthorhombic | orthorhombic | monoclinic |
| space group | $P2_1$ | $P2_12_12_1$ | $P2_12_12_1$ | $P2_1$ |
| cryst size, mm | 1.00 × 0.40 × 0.25 | 0.60 × 0.40 × 0.15 | 0.30 × 0.20 × 0.15 | 0.85 × 0.85 × 0.65 |
| $a$ (Å) | 15.0550(2) | 9.8938(1) | 9.8877(1) | 11.0122(2) |
| $b$ (Å) | 5.8540(1) | 10.2598(1) | 10.1558(2) | 11.9486(2) |
| $c$ (Å) | 23.4593(3) | 44.2594(6) | 37.7904(8) | 17.6226(3) |
| $\beta$ (deg) | 106.8839(4) | 90.00 | 90.00 | 105.8160(6) |
| $V$ (Å$^{3)}$ | 1978.39(5) | 4492.70(9) | 3794.8(1) | 2231.00(7) |
| $Z$ | 2 | 4 | 4 | 2 |
| $D_{calcd}$ (g/cm$^3$) | 1.183 | 1.260 | 1.181 | 1.163 |
| $\mu$(Mo K$\alpha$) (cm$^{-1}$) | 1.22 | 2.93 | 1.22 | 1.13 |
| total reflns | 6325 | 5384 | 6539 | 7255 |
| reflns with $I > 2\sigma I$ | 5902 | 4713 | 4698 | 6495 |
| $R^a$ | 0.0534 | 0.0503 | 0.0733 | 0.0346 |
| $R_w{}^b$ | 0.1461 | 0.1251 | 0.1649 | 0.0792 |

[a] $R = \sum||F_o| - |F_c||/\sum|F_o|$. [b] $R_w(F_o^2) = \{\sum w(F_o^2 - F_c^2)^2/\sum wF_o^4\}^{1/2}$.

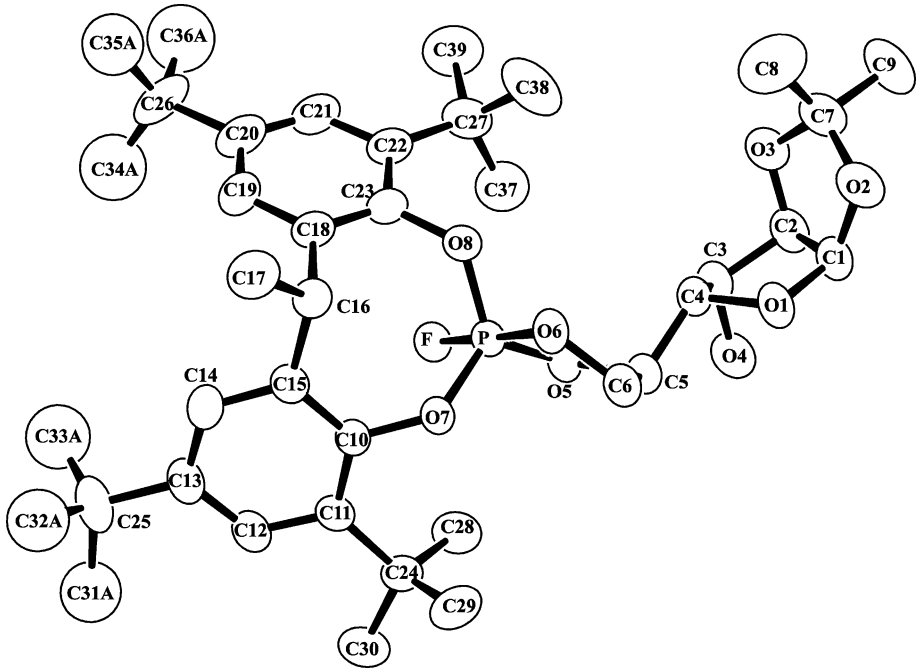


**Figure 1.** ORTEP diagram of **1A**. Only one set of the disordered *tert*-butyl group atoms is shown (with suffix "A").

**X-ray Studies.** The X-ray crystallographic studies were performed using a Nonius KappaCCD diffractometer and graphite monochromated Mo K$\alpha$ radiation ($\lambda$ = 0.710 73 Å). Data were collected at 293 K and $\theta_{MoK\alpha} \leq 25°$ (for **1**, **3**, and **4**) or $\theta_{MoK\alpha} \leq 22°$ (for **2**). All of the data were included in the refinement. The structures were solved by direct methods and difference Fourier techniques and were refined by full-matrix least-squares methods. Refinements were based on $F^2$, and computations were performed on a 2.6 GHz Pentium 4 computer using SHELXS-86 for solution[20] and SHELXL-97 for refinement.[21] All of the non-hydrogen atoms were refined anisotropically. Two of the *tert*-butyl groups in **1** were disordered, and they were refined in two positions with a 60:40 occupancy ratio at the isotropic level. There was a fairly well-behaved acetone molecule in the crystal lattice of **2**. One of the *tert*-butyl groups in **2** and **3** and the furanyl oxygen in **3** were disordered. They were refined in two positions with equal occupancy at the isotropic level. All hydrogen atoms were included in the refinement as isotropic scatterers riding in either ideal positions or with torsional refinement (in the case of methyl hydrogen atoms) on the bonded atoms. The hydrogens on disordered atoms and on the atoms connected to the disordered atoms and the OH group of **1** were not included in the calculations. The final agreement factors are based on the reflections with $I \geq 2\sigma_I$.

## Results and Discussion

Crystallographic data are summarized in Table 1. The atom-labeling schemes for **1**−**4** are given in the ORTEP plots of Figures 1−4, respectively. These figures were made using the ORTEP-III for Windows program.[22] The hydrogen atoms are omitted for clarity. The thermal ellipsoids are shown at the 50% probability level. Selected bond parameters are given in Tables 2−5.

(20) Sheldrick, G. M. *Acta Crystallogr., Sect. A* **1990**, *46*, 467−473.
(21) Sheldrick, G. M. *SHELXL-97*; University of Gottingen: Gottingen, Germany, 1997.
(22) Farrugia, L. J. *J. Appl. Crystallogr.* **1997**, *30*, 565−565.

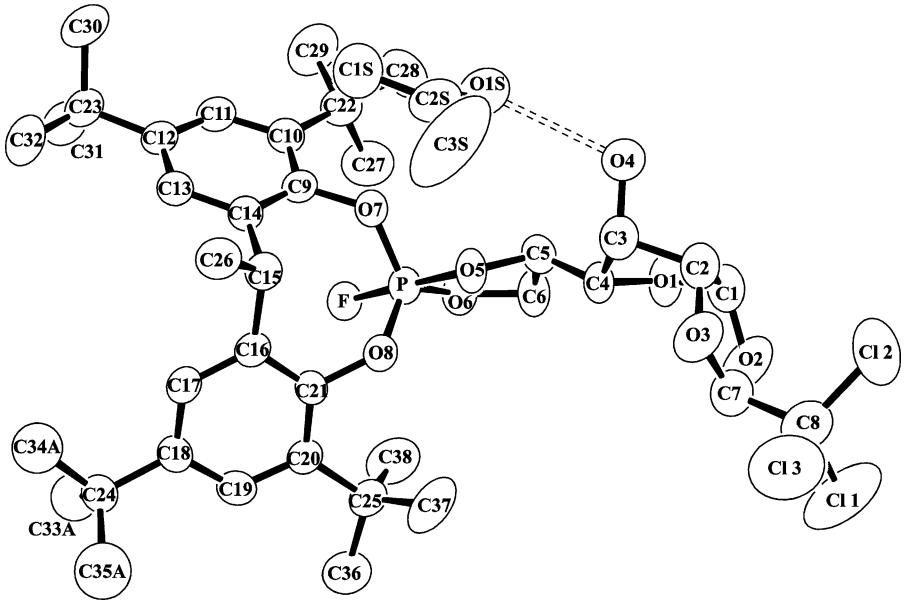


**Figure 2.** ORTEP diagram of **2B·acetone**. Only one set of the disordered *tert*-butyl group atoms is shown (with suffix "A"). Hydrogen bonding is shown with a dashed bond.

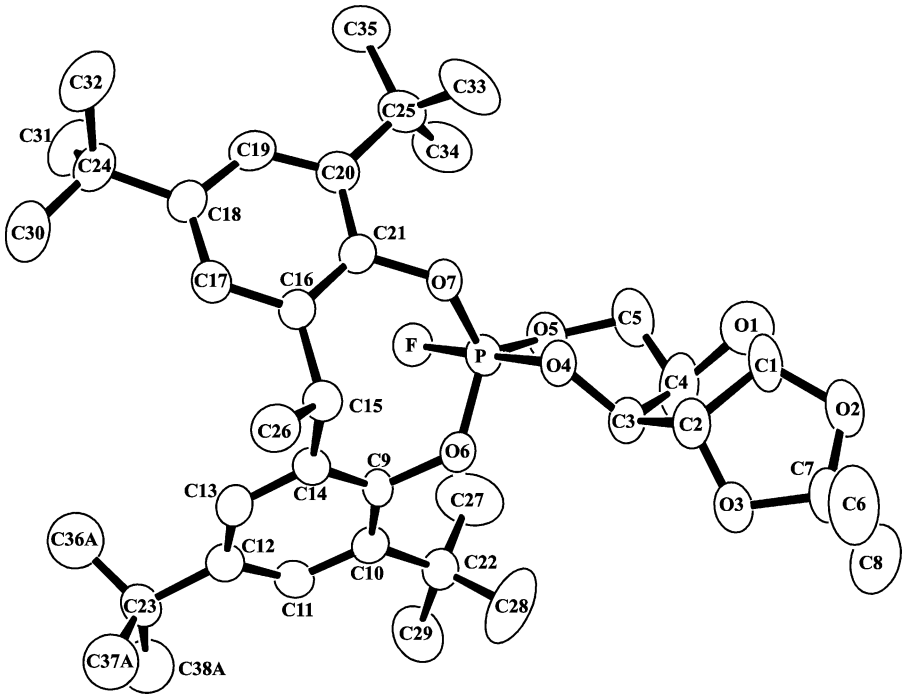


**Figure 3.** ORTEP diagram of **3B**. Only one set of the disordered *tert*-butyl group atoms is shown (with suffix "A"). Only one of the two O1 positions is shown.

**Syntheses.** The carbohydrate-based phosphoranes were synthesized by reacting the monocyclic fluorophosphite **A** (for **1**−**3**) or the acyclic phosphite **5** (for **4**) with the appropriate carbohydrate derivative in the presence of N-chlorodiisopropylamine in dichloromethane (Schemes 2−5). Even though $\beta$-chloralose was used in the synthesis of **2** (Scheme 3), the product contains the α-chloralose moiety, which is likely due to the isomerization of the chloral moiety. The reaction of the xylofuranose derivative took only a few hours in dichloromethane, whereas in ether, it did not reach completion even after 6 days, even though all of the reagents dissolved readily. Phosphorane **1** is very stable to water in ethanol and can be crystallized at ambient conditions from boiling acetonitrile (commercial grade). The hydroxyl group and P−F bond in **1** do not react at ambient conditions over several days, even when dissolved in triethylamine or pyridine. This shows that it is one of the very stable phosphoranes. Phosphoranes **2** and **3** are stable to water in ether and dichloromethane. However, they undergo slow hydrolysis in moist acetonitrile even at room temperature. Unlike the bicyclic phosphoranes **1**−**3**, the monocyclic phosphorane **4**, which contains no bulky *tert*-butyl groups, is fairly sensitive. Even pure single crystals of **4** completely decompose in the air in about 5 days, turning to an oil. This is the most sensitive of the eight biorelevant phosphoranes we have structurally characterized so far. This suggests that

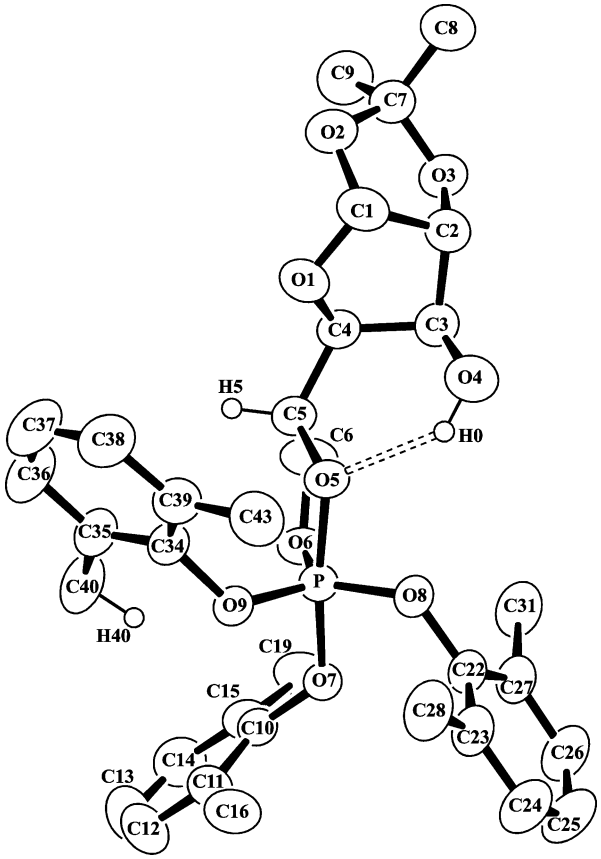


**Figure 4.** ORTEP diagram of **4**. The isopropyl terminal methyl carbons (at C16, C19, C28, C31, C40, and C43) are omitted for clarity. Hydrogen bonding is shown with a dashed bond. Only significant hydrogen atoms used in the discussion are shown.

**Table 2.** Selected Bond Lengths (Å) and Angles (deg) for **1**

| | | | |
|---|---|---|---|
| P−F | 1.605(2) | P−O(5) | 1.608(2) |
| P−O(6) | 1.652(2) | P−O(7) | 1.604(2) |
| P−O(8) | 1.598(2) | | |
| F−P−O(5) | 87.3(1) | F−P−O(6) | 177.7(1) |
| F−P−O(7) | 91.7(1) | F−P−O(8) | 91.5(1) |
| O(5)−P−O(6) | 91.8(1) | O(5)−P−O(7) | 116.6(1) |
| O(5)−P−O(8) | 121.9(1) | O(6)−P−O(7) | 90.5(1) |
| O(6)−P−O(8) | 87.2(1) | O(7)−P−O(8) | 121.5(1) |
| C(5)−O(5)−P | 114.6(2) | C(6)−O(6)−P | 111.5(2) |
| C(10)−O(7)−P | 127.6(2) | C(23)−O(8)−P | 126.0(2) |

**Table 3.** Selected Bond Lengths (Å) and Angles (deg) for **2·Acetone**

| | | | |
|---|---|---|---|
| P−F | 1.612(2) | P−O(5) | 1.657(3) |
| P−O(6) | 1.604(3) | P−O(7) | 1.593(3) |
| P−O(8) | 1.583(3) | | |
| F−P−O(5) | 178.0(2) | F−P−O(6) | 86.3(1) |
| F−P−O(7) | 91.7(1) | F−P−O(8) | 92.1(1) |
| O(5)−P−O(6) | 92.0(2) | O(5)−P−O(7) | 90.0(2) |
| O(5)−P−O(8) | 88.0(2) | O(6)−P−O(7) | 119.9(2) |
| O(6)−P−O(8) | 121.6(2) | O(7)−P−O(8) | 118.5(2) |

either the bicyclic system or the bulky *tert*-butyl groups or both act to increase the stability considerably.

**Structure and Isomerism in the Bicyclic Phosphoranes.** In the bicyclic phosphoranes **1**−**3**, the eight-membered ring occupies diequatorial positions of a trigonal bipyramid. Analogous eight-membered rings in bicyclic systems are known to occupy either diequatorial positions[23,24] or axial−equatorial positions[24,25] despite the presence of bulky groups. The smaller rings occupy axial−equatorial positions, as normally expected.

**Table 4.** Selected Bond Lengths (Å) and Angles (deg) for **3**

| | | | |
|---|---|---|---|
| P−F | 1.617(3) | P−O(4) | 1.658(3) |
| P−O(5) | 1.589(3) | P−O(6) | 1.607(3) |
| P−O(7) | 1.587(3) | | |
| F−P−O(4) | 177.7(2) | F−P−O(5) | 86.7(2) |
| F−P−O(6) | 90.9(2) | F−P−O(7) | 91.4(2) |
| O(4)−P−O(5) | 94.5(2) | O(4)−P−O(6) | 90.4(2) |
| O(4)−P−O(7) | 86.3(2) | O(5)−P−O(6) | 116.6(2) |
| O(5)−P−O(7) | 121.1(2) | O(6)−P−O(7) | 122.3(2) |
| C(3)−O(4)−P | 117.6(3) | C(5)−O(5)−P | 123.2(3) |
| C(9)−O(6)−P | 126.8(3) | C(21)−O(7)−P | 126.9(3) |

**Table 5.** Selected Bond Lengths (Å) and Angles (deg) for **4**

| | | | |
|---|---|---|---|
| P−O(5) | 1.6976(13) | P−O(6) | 1.606(1) |
| P−O(7) | 1.6615(12) | P−O(8) | 1.608(1) |
| P−O(9) | 1.5984(13) | | |
| O(5)−P−O(6) | 89.89(6) | O(5)−P−O(7) | 173.34(7) |
| O(5)−P−O(8) | 84.62(6) | O(5)−P−O(9) | 94.11(7) |
| O(6)−P−O(7) | 90.09(6) | O(6)−P−O(8) | 124.59(7) |
| O(6)−P−O(9) | 116.90(7) | O(7)−P−O(8) | 89.90(6) |
| O(7)−P−O(9) | 91.84(6) | O(8)−P−O(9) | 118.48(7) |

In phosphoranes **1**−**3** (Schemes 2−4), the eight-membered ring has an anti conformation as we have seen in many similar phosphoranes.[23] In this case, the two axial positions become nonequivalent. We name these two positions endo-axial and exo-axial (see schematic below). The endo-axial position is pointing to the inside of the eight-membered ring system. It is in the middle of the aromatic ring currents and is more sterically crowded. The exo-axial position is pointing outward of the eight-membered ring system and is mostly steric-free. Similarly, the methyl group also can have two orientations. The equatorial orientation at the bridging carbon has less of a steric factor, and hence, this position is preferred by the bulkier groups (in this case, the methyl group).

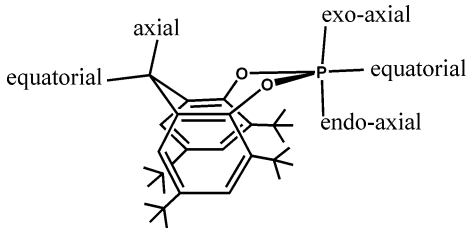


Because of the nonequivalence of available positions, phosphoranes **1**−**3** also show isomerism. There are two types of oxygen atoms in the carbohydrate moiety that bind to phosphorus. One is the least bulky primary oxygen (C−$CH_2O$), while the other is the bulkier secondary oxygen atom ($C_2CHO$). Either one can occupy one axial and one equatorial position. However, both seem to occupy the exo-axial or equatorial position without much steric influence. The orientation with the least steric group occupying the axial position was confirmed earlier in two model phosphoranes

(23) (a) Timosheva, N. V.; Chandrasekaran, A.; Prakasha, T. K.; Day, R. O.; Holmes, R. R. *Inorg. Chem.* **1996**, *35*, 6552−6560. (b) Timosheva, N. V.; Prakasha, T. K.; Chandrasekaran, A.; Day, R. O.; Holmes, R. R. *Inorg. Chem.* **1995**, *34*, 4525−4526. (c) Prakasha, T. K.; Chandrasekaran, A.; Day, R. O.; Holmes, R. R. *Inorg. Chem.* **1995**, *34*, 1243−1247. (d) Chandrasekaran, A.; Day, R. O.; Holmes, R. R. *J. Am. Chem. Soc.* **1997**, *119*, 11434−11441.

(24) Kommana, P.; Kumar, N. S.; Vittal, J. J.; Jayasree, E. G.; Jemmis, E. D.; Swamy, H. C. K. *Org. Lett.* **2004**, *6*, 145−148.

(25) Said, M. A.; Pulm, M.; Irmer, R. H.; Swamy, K. C. K. *Inorg. Chem.* **1997**, *36*, 2044−2051.

**Scheme 2**

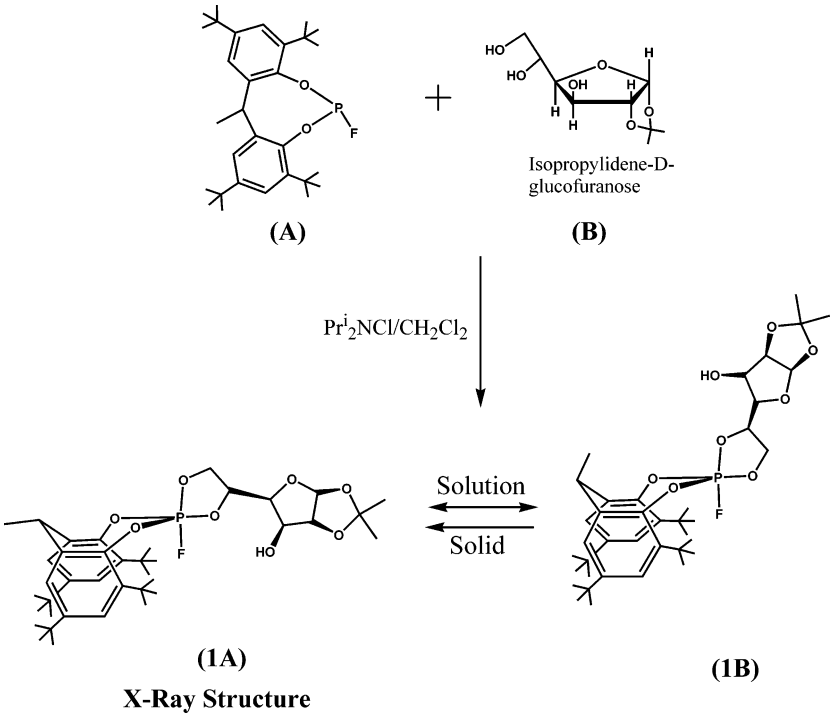


**Scheme 3**

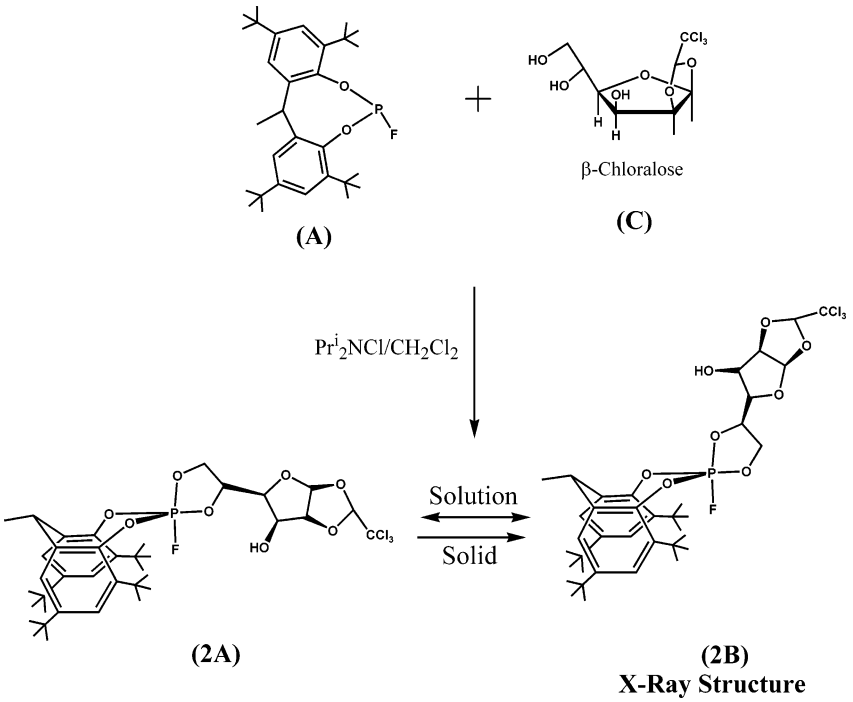


where the rings were fused with a trans orientation,[26,27] whereas in the case of **3**, the xylofuranose moiety has a cis orientation at the ring fusion. This study confirms that both orientations with the bulkier alkoxy at an axial or equatorial position are easily possible, and hence, it is expected that the energy difference between these two orientations is small. Phosphoranes **1**−**3** show a dynamic equilibrium involving two isomers in solution. In the solid state, one of these two isomers is present. In contrast, only one isomer exists in solution for phosphorane **6**, and that isomer is different from the one shown in the solid state.[1b]

In the recently reported thymidine-based phosphorane **6** (Scheme 1),[1b] the $POCH_2$ protons resonated at 2.40 and 2.57 ppm, whereas in **1**−**3**, all OCH protons resonate above 4 ppm. This absence of any upfield shift for these protons further confirms the assignment that no OCH group is in the endo-axial position in all six of the isomers of **1**−**3**. The

(26) Yu, J. H.; Arif, A. M.; Bentrude, W. G. *J. Am. Chem. Soc.* **1990**, *112*, 7451−7461.
(27) Holmes, R. R.; Swamy, K. C. K.; Holmes, J. M.; Day, R. O. *Inorg. Chem.* **1991**, *30*, 1052−1062.

**Scheme 4**

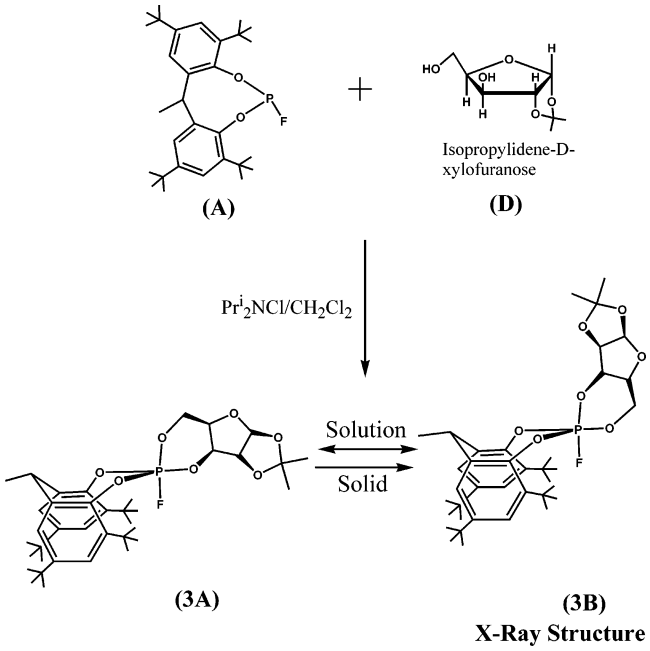


P−F coupling for the equatorial bond in a tetraoxyphosphorane was observed to be 922.5 Hz.[28] In all of the isomers of phosphoranes **1**−**3**, the values were far lower (on the order of 770 Hz), confirming their axial placement as observed in the X-ray study.

The eight-membered rings in the bicyclic phosphoranes **1**−**3** have an ideal boat-chair (anti) conformation. Figure 5 depicts this for **1** along with the orientation of substituents at the phosphorus. The six-membered ring in **3** (Figure 6) has a boat conformation with the axial oxygen O4 and the opposite carbon C5 deviating from the plane formed by the other four atoms (by 0.66 and 0.56 Å, respectively). The six-membered ring in the thymidine-based phosphorane **6** also has a boat conformation with the axial oxygen atom and the opposite carbon atom deviating from the plane formed by the other four atoms (by 0.56 and 0.67 Å, respectively). The five-membered phosphorus heterocycles for **1**−**4** are twisted, as seen from the Figures 1−4. The methylene carbon C6 deviates most from planarity in **1**, whereas the methyne carbon C5 deviates most in **2** and **4**.

**Dynamic Equilibrium in Bicyclic Phosphoranes.** The NMR data suggest that there is a dynamic equilibrium in solution between two different isomers. The activation energy for this process for **1** and **3** was calculated to be 64.4 and 73.6 kJ/mol (15.4 and 17.6 kcal/mol), respectively, from an analysis of variable-temperature $^{31}P$ NMR spectra. A monocyclic phosphorane with the identical bridging system and trifluoroethoxy groups occupying the remaining three positions of the trigonal bipyramid had a similar activation energy for ring inversion, that is, 15.4 kcal/mol.[29] The high activation energy is most likely due to the presence of the bulky *tert*-butyl groups. The retention of fluorine in the endo-axial position suggests that this is not the simple ring inversion we observed in a comparable silicon system.[30] By that we mean that, in this system, a simple ring inversion will invert the orientations at phosphorus and at the carbon bridging the aryl rings.

It is instructive to summarize the results from the NMR studies first and then give the more-detailed discussion. The NMR changes due to reorientation in the eight-membered ring are caused by the presence of the asymmetric CHMe group and will reflect if ring inversion is present or not in **1**−**3**. Reorientation of the groups at phosphorus can occur if there is ring inversion in this system or by a fluxional process, which we will assume is the Berry pseudorotation process.[6,7] The reorientation at phosphorus does not necessitate a ring inversion in the eight-membered ring part. Thus, of the two processes that can cause the orientation changes, an eight-membered ring inversion will lead to orientation changes at both C and P. However, Berry pseudorotation will lead to orientation changes only at P without any change at C. If two ring inversions accompany the latter process, this will not be differentiated from the absence of any ring inversion. As given in more detail below, the interconversion of **1A** to **1B** involves both of the above processes, but the interconversion of **2A** to **2B**, **3A** to **3B**, and **6A** to **6B** proceeds only by the Berry pseudorotation process.

**Detailed NMR Discussion.**[31] The high-energy fluxional process is expected to involve Berry pseudorotation, with or without the eight-membered ring inversion, and results in the exchange of positions for primary and secondary alkoxy groups (C−$CH_2$O and $C_2$CHO, respectively). The positional change of the methyl group in **1B** (see Scheme 2) suggests ring inversion. As seen from the crystal structures of **1**−**3**, the alkoxy groups can be placed at either an axial or an equatorial position because the energy difference is not expected to be high. In addition, the proton NMR spectra for **1** and **3**, even at −60 °C (in $CDCl_3$ and $CD_2Cl_2$), give too many broad peaks that are complicated. This affects only the protons of the carbohydrate moiety attached to C2−C6 in the case of **1** and to C2−C5 in case of **3**. This is presumably due to a low-energy fluxional process, such as rotation around the C4−C5 single bond in case of **1** and the conformation changes for the six-membered ring in the case of **3**. Only the low-temperature NMR data for phosphorane **1** at −50 °C are provided because this shows that the hydroxyl protons (including traces of water) shift downfield compared to room temperature. The assignment of the hydroxyl protons is based on this shift of about 0.6 ppm (0.5 ppm for water) and the correlation observed in the correlation spectroscopy (COSY) experiment for this peak with those of carbohydrate protons.

(28) Meyer, T. G.; Fischer, A.; Jones, P. G.; Schmutzler, R. *Z. Naturforsch., B: Chem. Sci.* **1993**, *48*, 659−671.
(29) Abdou, W. M.; Denney, D. B.; Denney, D. Z.; Pastor, S. D. *Phosphorus Sulfur Relat. Elem.* **1985**, *22*, 99−107.
(30) Chandrasekaran, A.; Day, R. O.; Holmes, R. R. *Organometallics* **1996**, *15*, 3189−3197.
(31) Actually, there are eight possible isomers or conformations for each of **1**, **2**, **3**, or **6**, though two of them can be sterically least feasible. We see only two forms in each phosphorane. We have observed four forms in total, when we compare **1**, **2**, **3**, and **6**. Form 1 is the most stable on the basis of the steric factors or group sizes. In all forms, the eight-membered ring is considered to be in the most stable diequatorial positions with an anti form.

**Scheme 5**

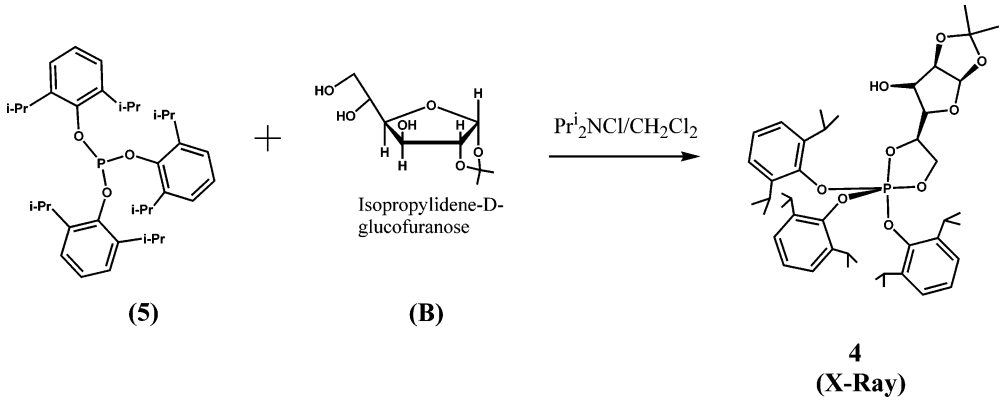


The isomers **A** are similar in **1**−**3**, while **2B** and **3B** are similar to each other (see Table 6). However, **1B** is somewhat different than **2B** and **3B**, as evidenced from the proton and carbon NMR data given below. First, the fluorine NMR data suggest that the position of the fluorine remains the same in all isomers. The phosphorus NMR data suggest that not much difference exists between the isomers, as seen from the insignificant changes in chemical shift and $J_{P-F}$ couplings between isomers **A** and **B**. The proton and carbon NMR spectra offer insights into the changes that happen in other parts of the molecule, away from the central phosphorus.

The proton NMR spectra were rather difficult to assign completely because of the fluxional processes described earlier. Only the protons from the eight-membered ring system, the proton at C1, and the protons of the isopropyl group were easy to identify. The only difference in the eight-membered ring system among the six isomers of **1**−**3** is the orientation of the substituents (H/Me) at the bridging carbon ($Ar_2CHMe$). In isomer **1B**, the Me group is placed in the higher-energy axial position, whereas it occupies the most preferred equatorial position in all of the other isomers. This is seen from the huge chemical shift difference for the CH proton, which resonates at 4.8−4.9 ppm for **1A**, **2A**/**2B**, and **3A**/**3B**. For **1B**, it resonates at 3.37 ppm, which was confirmed to couple with one of the $CH_3$ doublets by a COSY experiment. The other doublets show a correlation to the resonance at 4.9 ppm. The $CH_3$ protons resonate at 1.66−1.68 ppm for **1A**, **2A**, **2B**, **3A**, and **3B**. The $CH_3$ protons resonate at 1.46 ppm for **1B**, suggesting a change in the environment for this methyl group.

**Table 6.** Eight Possible Forms for **1**, **2**, **3**, and **6**[a]

| form | example | $CH_3$ at $CAr_2$ | F | primary O | secondary O |
|---|---|---|---|---|---|
| 1 | **1A**, **2A**, **3A**, **6A** | **equatorial** | **endo-axial** | **exo-axial** | **equatorial** |
| 2 | **2B**, **3B** | **equatorial** | **endo-axial** | equatorial | exo-axial |
| 3 | **6B** | **equatorial** | exo-axial | endo-axial | equatorial |
| 4 | **1B** | axial | **endo-axial** | equatorial | exo-axial |
| 5 | none | axial | **endo-axial** | **exo-axial** | **equatorial** |
| 6 | none | axial | exo-axial | endo-axial | **equatorial** |
| 7* | none | **equatorial** | exo-axial | equatorial | endo-axial* |
| 8* | none | axial | exo-axial | equatorial | endo-axial* |

[a] The most stable orientations are shown in bold. Sterically least-favored forms are shown with an asterisk.

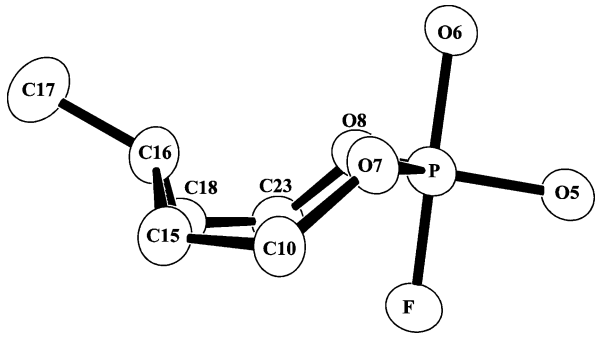


**Figure 5.** ORTEP diagram of **1A** showing the eight-membered ring boat conformation with the orientation of substituents at phosphorus and the opposite carbon atom C17.

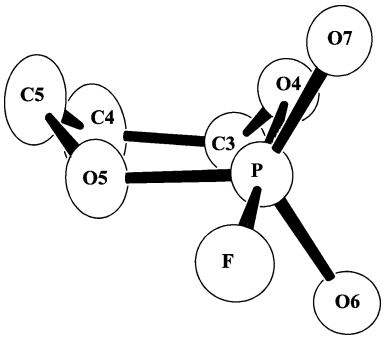


**Figure 6.** ORTEP diagram of **3B** showing the six-membered ring conformation with the orientation of substituents at phosphorus.

The change of positions for the primary and secondary alkoxy groups were clearly evidenced by the $^{13}C$ NMR spectra. The primary $OCH_2$ carbon atoms were identified by $^{13}C$ distortionless enhancement by polarization transfer experiments and show two signals for each compound, separated by about 4.0 ppm in **1** and 2.9 ppm in **3**. The secondary OCH carbon atoms were identified by the large coupling with phosphorus (10.8 and 17.3 Hz for **1** and **3**, respectively, in the equatorial positions and 5.4 and 14.0 Hz for **1** and **3**, respectively, in the axial positions) and also by the appearance of two signals for each compound separated by about 1.4 ppm in **1** and 3.1 ppm in **3**. The lower coupling values observed with the five-membered ring system of **1** can be explained as a result of competing couplings $^2J_{POC}$ and $^3J_{POCC}$ from opposite directions, which also results in no observable coupling value for the primary $OCH_2$ carbon.

The chiral nonsymmetric five- or six-membered rings attached to phosphorus create an asymmetric environment for the eight-membered ring system. As a result, the *tert*-

butyl carbons and protons closer to the phosphorus atom and the protons attached to the aromatic ring all show asymmetry. The effect is clearer in the case of **3** where two fused five-membered rings are also fused to the six-membered ring and are more pronounced in case of **3A** because these fused rings are placed much closer to the eight-membered ring.

**Structure and Hydrogen Bonding in the Monocyclic Phosphorane.** The X-ray structure of phosphorane **4** reveals that it is very similar to phosphorane **7**, which we reported recently.[1b] In both cases, the five-membered ring occupies axial−equatorial positions of a trigonal bipyramid and the bulkier secondary oxygen occupies the axial position. An important difference is that there is intramolecular hydrogen bonding in **4**, whereas in **7**, the hydroxyl group was hydrogen bonded with a solvent ether molecule. The details of this difference are discussed below.

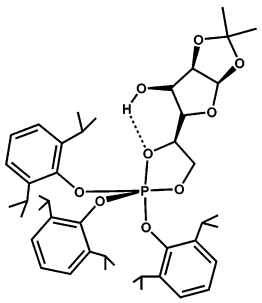

**(4)**

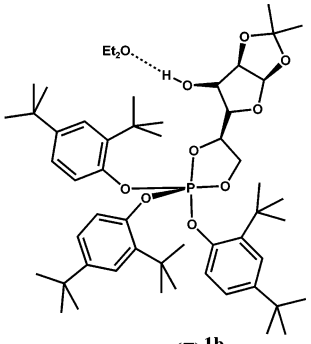

**(7)**[1b]

In phosphoranes **1**, **2**, **4**, and **7**, there is a free hydroxyl group, which can be involved in hydrogen bonding. However, in phosphorane **1**, the OH group does not participate in any hydrogen bonding. Phosphorane **2** readily forms hydrogen bonds with acetone (Figure 2) or ethanol, whereas phosphorane **7** exhibits hydrogen bonding with ether.[1b] The sensitive phosphorane **4** forms intramolecular hydrogen bonds to the axial oxygen atom O5 (Figure 4). A comparison of the axial P−O bond lengths of the phosphoranes reveals that the axial P−O bond length in **4** is the longest at 1.698(1) Å, whereas in all others, the axial bonds remain shorter than 1.67 Å. In phosphoranes **4** and **7**, the equatorial bonds have almost identical bond lengths. A variation of only 0.008 Å exists among the six bonds of both compounds. In **7**, both axial P−O bond lengths are identical at 1.669(4) Å. In sharp contrast, the axial P−O bond length in **4** for the secondary oxygen of $C_2CHO$ is considerably longer than the other axial P−O bond, by 0.036 Å. We attribute the major difference in these two axial bond lengths to the presence of the OH hydrogen bond for **4**. This close comparison in axial bond lengths between **4** and **7** shows that the hydrogen bond can weaken the normal P−O bonds. Earlier, we have shown that such weakening is possible for P−O donor bonds.[5] In some models, such hydrogen bonds weakening P−O bonds have been proposed but not confirmed with structural evidence.[32]

(32) (a) Jubian, V.; Veronese, A.; Dixon, R. P.; Hamilton, A. D. *Angew. Chem., Int. Ed. Engl.* **1995**, *34*, 1237−1239. (b) Bruice, T. C.; Blasko, A.; Arasasingham, R. D.; Kim, J.-S. *J. Am. Chem. Soc.* **1995**, *117*, 12070−1207. (c) Blasko, A.; Bruice, T. C. *Acc. Chem. Res.* **1999**, *32*, 475−484.

The proton NMR of **4** shows that the molecule is fluxional, especially in the aryl and isopropyl groups. The carbohydrate moiety shows sharp signals most likely because of fast averaging. The low-temperature NMR data show that the single broad peak of isopropyl protons separates into several individual peaks. There are six isopropyl groups, but at least seven individual methyl doublets can be seen in addition to some unresolved peaks. This suggests that there is anisotropy within each isopropyl group resulting in nonequivalence for the methyl protons, and at low temperatures, free rotation is hindered. In addition, the low-temperature NMR spectra also show that there is high shielding for some methyl doublets. The latter resonate at 0.35 and 0.77 ppm at 213 K for **4**, whereas the methyl protons all resonate as a broad peak in the range of 1.0−1.2 ppm and at 1.08 ppm in phosphite **5** at 295 K. Most likely, the high-field methyl shifts for **4** are due to the close proximity of the protons to the aromatic ring currents in the crowded environment.

An examination of the crystal structure of **4** supports this assertion. There are some protons placed very close to the aromatic rings (these protons are shown in Figure 4). The hydrogen atom H5 (attached to C5) is only 2.73 Å from the aromatic carbon C34, and the H40 proton (attached to the isopropyl carbon C40) is only 2.61 Å from the aromatic carbon C10. Thus, the NMR spectra show that the solution structure at low temperatures has a high probability of resembling the solid state structure, accompanied by slow fluxionality.

**Biochemical Implications.** In previous work in our laboratory, studies on model five- and six-coordinated phosphorus compounds demonstrated that factors prevalent at active sites of phosphoryl transfer enzymes, particularly donor coordination from residues, supported increased enzymatic activity. The present work establishes two additional factors that are important considerations governing enzymatic activity. The NMR studies reported here on newly characterized biorelevant species show conclusively that hydrogen bonding at an oxygen atom situated at an apical position of a trigonal bipyramid is capable of causing accelerated P−O bond cleavage due to the structurally observed increase in the P−O bond distance. As a consequence, product formation from the activated state is enhanced.

Additionally, in the area of promiscuous phosphoryl transfer enzymes, the work provides a mechanism for such enzymes to conduct different reactions at the same active site. For example,[9] chymotrypsin catalyzes the hydrolysis of a number of different substrates initiated by the attack of a serine residue at a carbon atom that is thought to lead to similar tetrahedral activated states. Chymotrypsin also catalyzes the reaction at a tetrahedral phosphoryl group that leads to a proposed trigonal bipyramidal activated state.[9] Thus, the active site of chymotrypsin is able to catalyze both amidase and phosphotriesterase reactions. The present work and our recent communication[1b] established the X-ray structure of several biorelevant phosphoranes **1**−**4**, **6**, and **7**. The bicyclic phosphoranes **1**−**3** and **6** exist in solution in equilibrium with an isomeric representation and exhibit a

dynamic exchange between their isomeric forms. The monocyclic phosphoranes **4** and **7** show fluxionality similar to that of the nonbiorelevant phosphoranes studied previously. Furthermore, the phosphoranes retain their structural integrity going from the solid state structures to solution. The rapid exchange process reorients the nucleotidyl or carbohydrate component of the trigonal bipyramidal phosphorane. At an active site, this type of pseudorotational behavior provides a mechanism that could bring another active site residue into play and accounts for a means for phosphoryl transfer enzymes to express promiscuous behavior. Pseudorotation, a well-founded process in nonenzymatic phosphorus chemistry,[6,7] may have an application in the future of phosphoryl transfer enzyme chemistry.

**Acknowledgment.** We thank the X-ray Structural Characterization Laboratory at the Chemistry Department supported by the University of Massachusetts and National Science Foundation (Grant CHE-9974648). Our sincere thanks are also due to NMR Director Dr. L. Charles Dickinson for recording the solid state $^{31}$P NMR spectra and helping in obtaining low-temperature and COSY NMR spectra.

**Supporting Information Available:** CIF files containing tables of atomic coordinates, anisotropic thermal parameters, bond lengths and angles, and hydrogen atom coordinates for **1**−**4**. This material is available free of charge via the Internet at http://pubs.acs.org.

IC052105E